



Universidade de São Paulo

Biblioteca Digital da Produção Intelectual - BDPI

Departamento de Astronomia - IAG/AGA

Comunicações em Eventos - IAG/AGA

2013

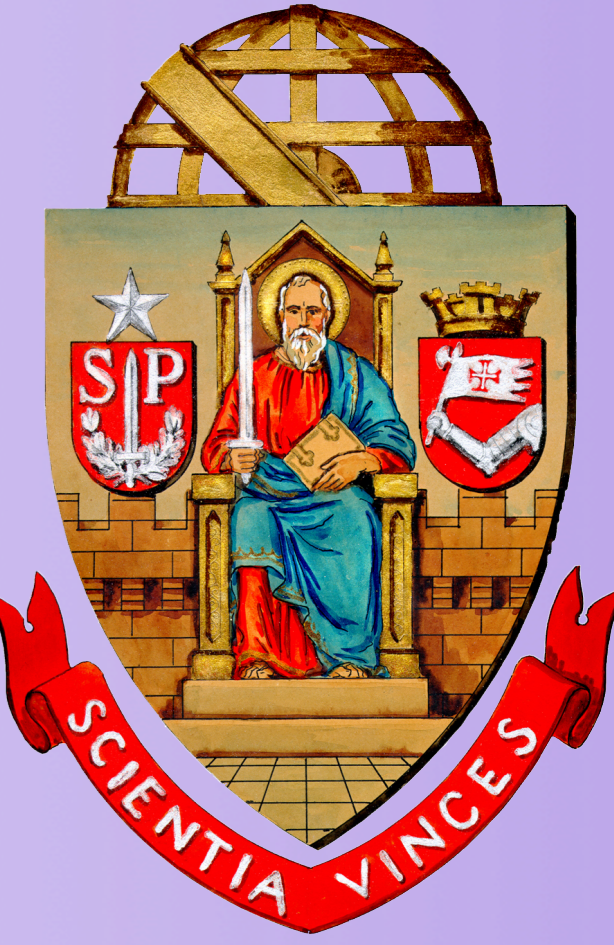
X-ray sources associated with young stellar objects in the star forming region CMaR1

Conference on Protostars and Planets, 6, 2013, Heidelberg
<http://www.producao.usp.br/handle/BDPI/44912>

Downloaded from: Biblioteca Digital da Produção Intelectual - BDPI, Universidade de São Paulo



X-RAY SOURCES ASSOCIATED WITH YOUNG STELLAR OBJECTS IN THE STAR FORMING REGION CMaR1



¹Thais dos Santos Silva, ¹Jane Gregorio-Hetem, ²Thierry Montmerle
¹Instituto de Astronomia Geofísica e Ciências Atmosféricas, Departamento de Astronomia
²Institut d'Astrophysique de Paris
thaisfi@astro.iag.usp.br

Abstract

In previous works we studied the star formation scenario in the molecular cloud Canis Major R1 (CMa R1), derived from the existence of young stellar population groups near the Be stars Z CMa and GU CMa, using data from the ROSAT X-ray satellite. In order to investigate the nature of these objects and to test a possible scenario of sequential star formation in this region, four fields (each 30 arcmin diameter, with some overlap – Fig. 1) have been observed with the XMM-Newton satellite, with a sensitivity about 10 times better than ROSAT.

The XMM-Newton data are currently under analysis. Preliminary results indicate the presence of about 324 sources, most of them apparently having one or more near-infrared counterparts showing typical colors of young stars. The youth of the X-ray sources was also confirmed by X-ray hardness ratio diagrams (XHRD), in different energy bands, giving an estimate of their L_X/L_{bol} ratios.

In addition to these results, we present a detailed study of the XMM field covering the cluster near Z CMa. Several of these sources were classified as T Tauri and Herbig Ae/Be stars, using optical spectroscopy obtained with Gemini telescopes, in order to validate the use of XHRD applied to the entire sample. This classification is also used to confirm the relation between the luminosities in the near-infrared and X-ray bands expected for the T Tauri stars in CMa R1. In the present work we show the results of the study based on the spectra of about 90 sources found nearby Z CMa. We checked that the X-ray spectra (0.3 to 10 keV) of young objects is different from that observed in field stars and extragalactic objects. Some of the candidates also have light curve showing flares that are typical of T Tauri stars, which confirms the young nature of these X-ray sources.

Introduction

The production of X-ray in star forming regions is associated with:

- ✦ Magnetic activity from lower mass pre-main sequence stars:
- ✦ Thermalization by high velocity winds from massive OB stars:
 - ✦ close to the star;
 - ✦ edges of a wind termination shock.
- ✦ Supernova remnants from past generation of OB stars. (Montmerle, et al. 2002)

Canis Majors Star Forming Region (CMaR1)

- ✦ Using data from the ROSAT X-ray satellite, having a field-of-view of $\sim 1^\circ$ in diameter, Gregorio-Hetem et al. (2009) discovered in this region young stellar objects mainly grouped in two clusters of different ages:
 - ✦ an older cluster ($> 10^7$ yr) in the neighborhood of GU CMa ($\sim 30'$ West of ionized nebula);
 - ✦ a younger cluster ($< 5 \times 10^6$ yr) nearby Z CMa.

In between these clusters it is found an intermediate population ($\sim 5 \times 10^6$ yr) of low mass stars. Our goal is to confirm, in the inter-cluster region (fields C and S), the mixture of both clusters members and the evidences of different star formation episodes.

Fields observed with XMM

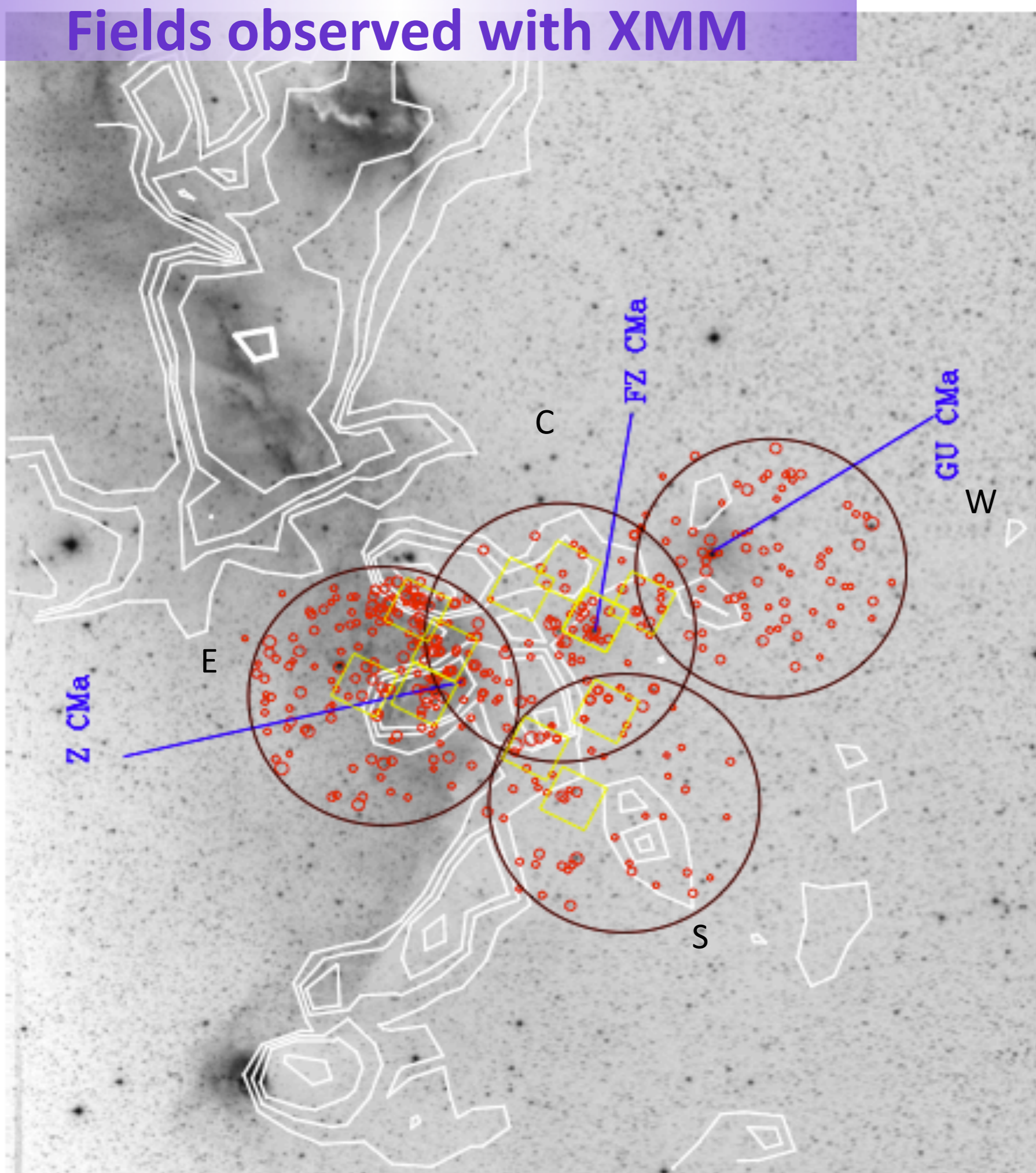


Fig.1. Observed fields with XMM-Newton. CMa R1 Optical image (DSS-R) superimposed by ^{12}CO contours showing the observed XMM-Newton fields (black circles - $15'$ radius). Red circle are X-ray sources. Gemini fields that have been observed in this year (yellow squares $6' \times 6'$).

X-ray observations and sources detection

- ✦ Four fields observed with PN, MOS1 and MOS2 EPIC camera from XMM-Newton satellite (Fig1.);
- ✦ 327 sources detected into all three different energy ranges based on Barrado et al 2011 (B2011), Lopez-Santiago et al. 2008 (LS208) and Hasinger et al. 2001 (H2001);

	IDet.	B1	B2	B3	B4	C	E	W	S	Total
	(keV)	(keV)	(keV)	(keV)	(keV)	(keV)	(sources)	(sources)	(sources)	(sources)
B2011	0.5 - 7.3	0.5 - 1.0	1.0 - 2.0	2.0 - 7.3	-	86	192	76	43	397
LS208	0.3 - 7.5	0.3 - 2.0	2.0 - 4.5	4.5 - 7.5	-	82	188	72	40	382
H2001	0.2 - 10.0	0.2 - 0.5	0.5 - 2.0	2.0 - 10	5.0 - 10	173	265	149	133	720

Tab. 1: Characteristic of detection sets based on different authors (B2011), (LS208) and (H2001): detection interval (IDet), used bands B1, B2, B3 and B4, and number of sources detected in each field - central (C) 07 02 58.40 -11 27 24.00, east (E) 07 04 18.34 -11 34 44.70, west (W) 07 01 23.00 -11 19 56.60, south (S) 07 02 29.51 -11 47 12.40, and total.

Hardness ratio diagrams

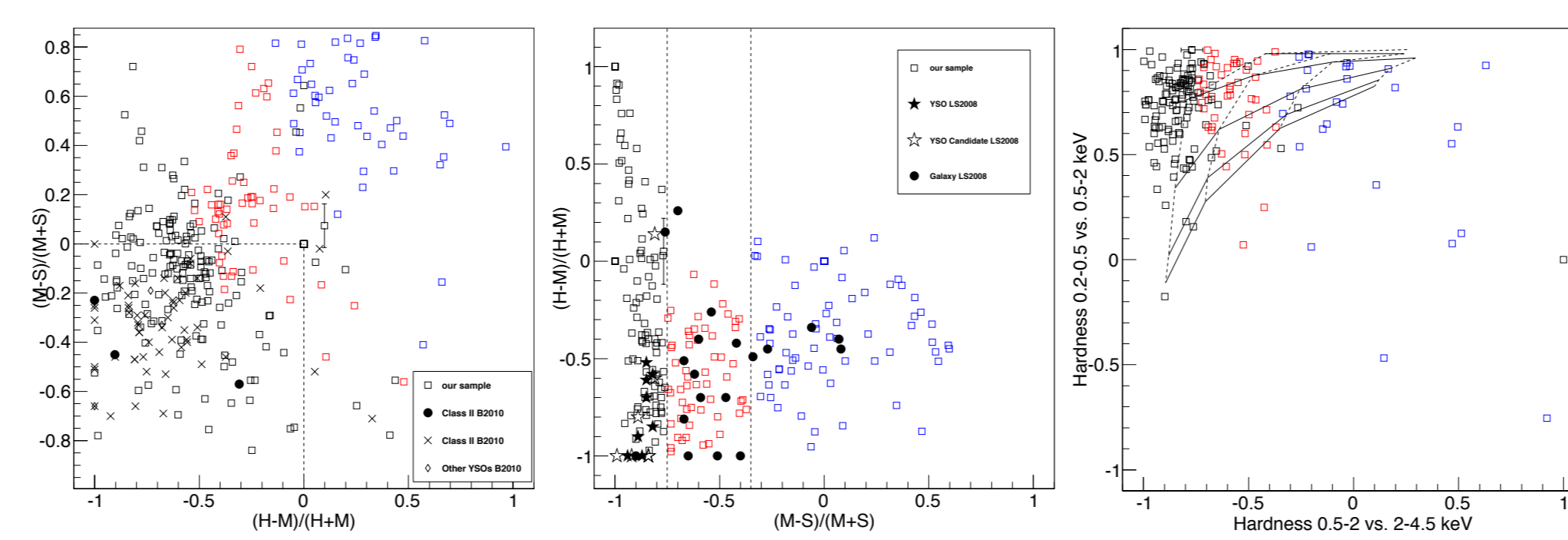


Fig.2. Hardness ratio diagrams based on three different range sets: (left) the dashed line delimits the region (smaller squares) where most of young objects of B2011, class II (filled circles), class III (crosses) and other young objects (diamond) are located: (center) the dashed line represents the locus of 90% of type 1 of XMM-Newton bright serendipitous survey sample (Della Ceca et al. 2004) with LS2008 sample, the YSOs and YSO candidates are represented by full and open stars, whereas the galaxy by circles. (right) grid of power law models presented in H2001. The objects detected in our 4 fields are represented by squares into the all diagrams. The different colours follow the limits proposed by Della Ceca et al. (2004), black symbols have hardness ratio (M-S)/(M-S) < -0.75, red symbols are in the type 1 AGN's regions and blue symbols are (M-S)/(M-S) > -0.35.

East field X-ray sample

In order to establish the analysis method of our whole sample we studied in more detail the optical, near infrared (NIR) and X-ray characteristics of about 50 of the brightest sources in the east field.

Optical and NIR analysis

Fernandes et al. 2013 (in preparation,) used GEMINI data to classify about 84 object present in our east field, based on this classification we could identify 24 X-ray sources:

- ✦ 6 \rightarrow weak T Tauri;
- ✦ 9 \rightarrow post T Tauri;
- ✦ 1 \rightarrow classical T Tauri;
- ✦ 1 \rightarrow Herbig Ae/Be;
- ✦ 1 \rightarrow YSO with emission line;
- ✦ 6 \rightarrow field objects.

Only two objects in our sample do not have 2MASS counterpart.

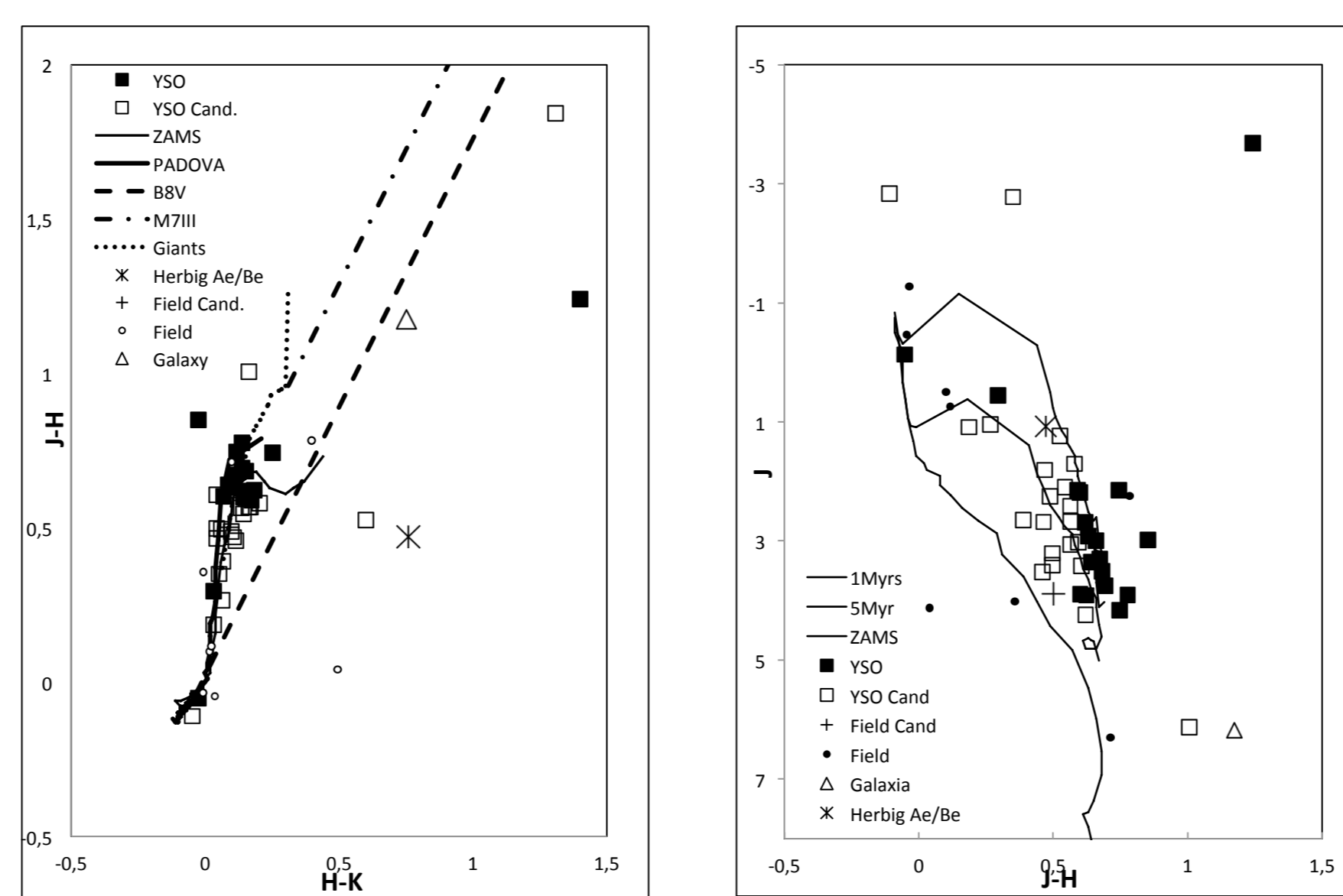


Fig.3. Left: colour-colour diagram. The main sequence and the ZAMS are indicated by full lines, while the locus of giant stars is represented by a dotted line. Reddening vectors from Rieke & Lebofsky (1985) are shown by dashed and dot-dashed lines. Right: colour-magnitude diagram showing the isochrones and evolutionary pre-MS tracks from Siess et al. (2000). The full and open squares represent the YSO and YSO candidate, crosses and dots are field candidate and field objects respectively, and the galaxy and the Herbig Ae/Be identified in our sample are respectively represented by open triangle and star.

X-ray analysis

Hardness ratio diagrams, in three different set energy for our sample compared with other works.

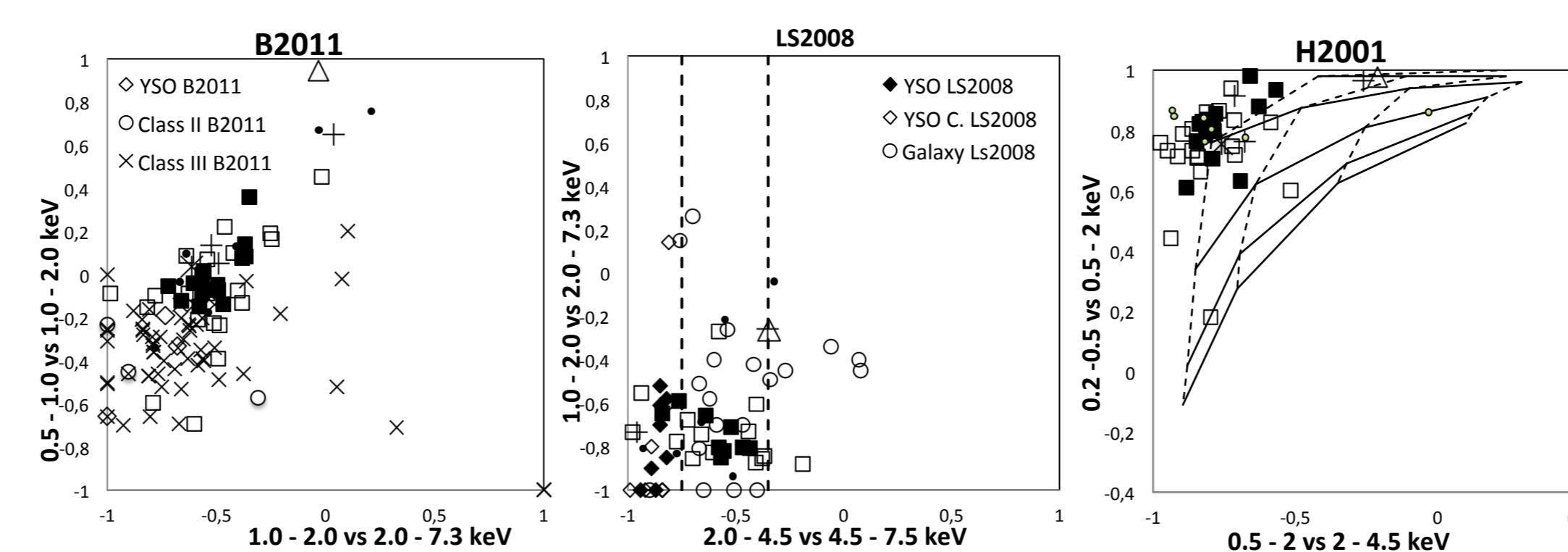


Fig.4. Hardness ratio diagrams similar to Fig.2, for a small sample in east field based on three different works. The full and open squares represent the YSO and YSO candidate, crosses and dots are field candidate and field objects respectively, and the galaxy and the Herbig Ae/Be identified in our sample are respectively represented by open triangle and star.

Different spectra present in our sample.

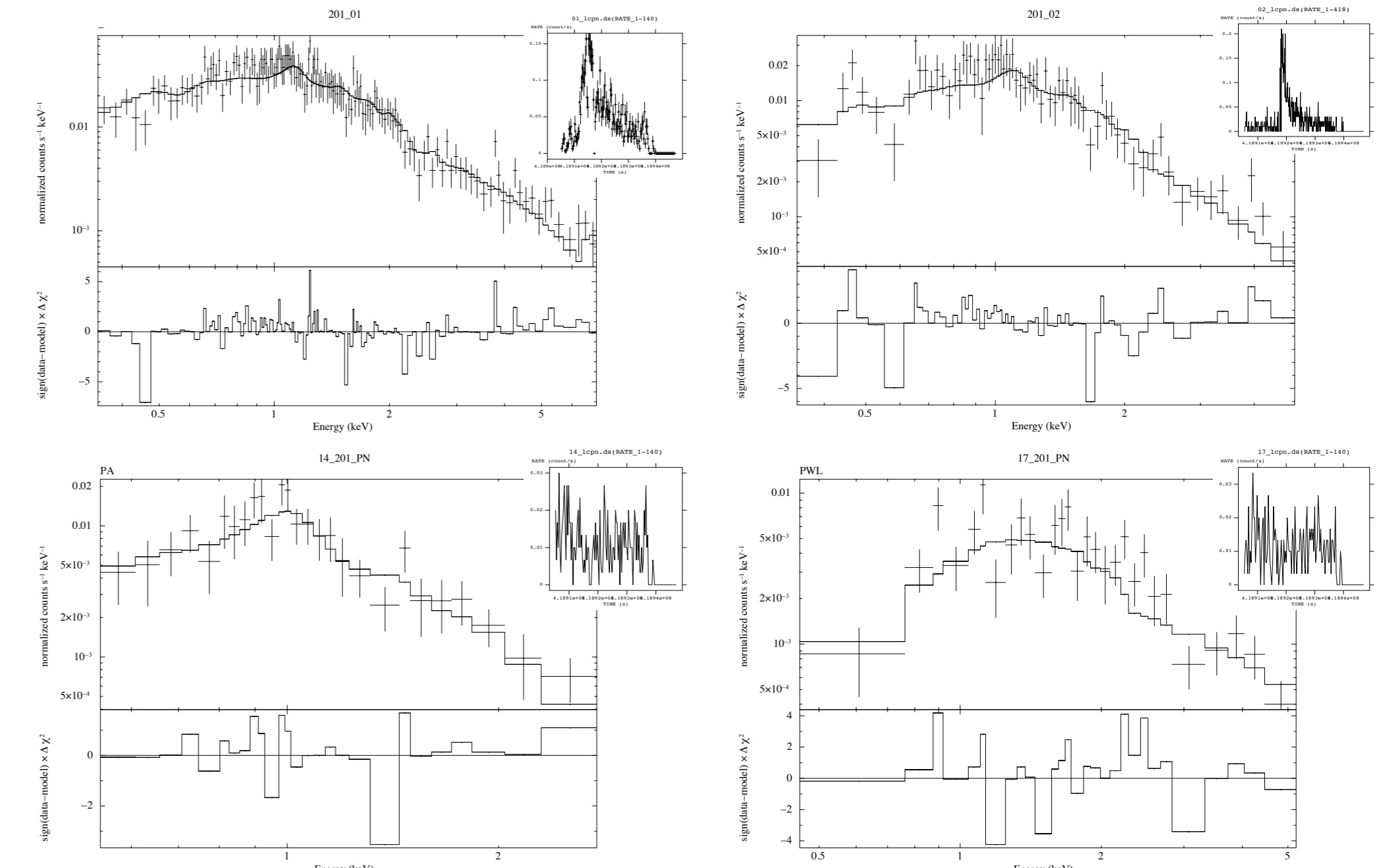


Fig.5. X-ray spectra example found in our sample. Top: Two of the brightest sources (01_201 and 02_201) in east field, both present a very strong flare. Bottom: (left) an example of a thermal plasma with one temperature component model fitted in a YSO source - 14_201, (right) a power law model example fitted in a field object - 17_201. In the right top of all spectra is the source light curve.

Using ROSAT data Gregorio-Hetem et al. (2009) found the relationship between NIR and X-ray luminosities for T Tauri stars in CMaR1 :

$$\log(L_X) = 31 - 0,33M_J$$

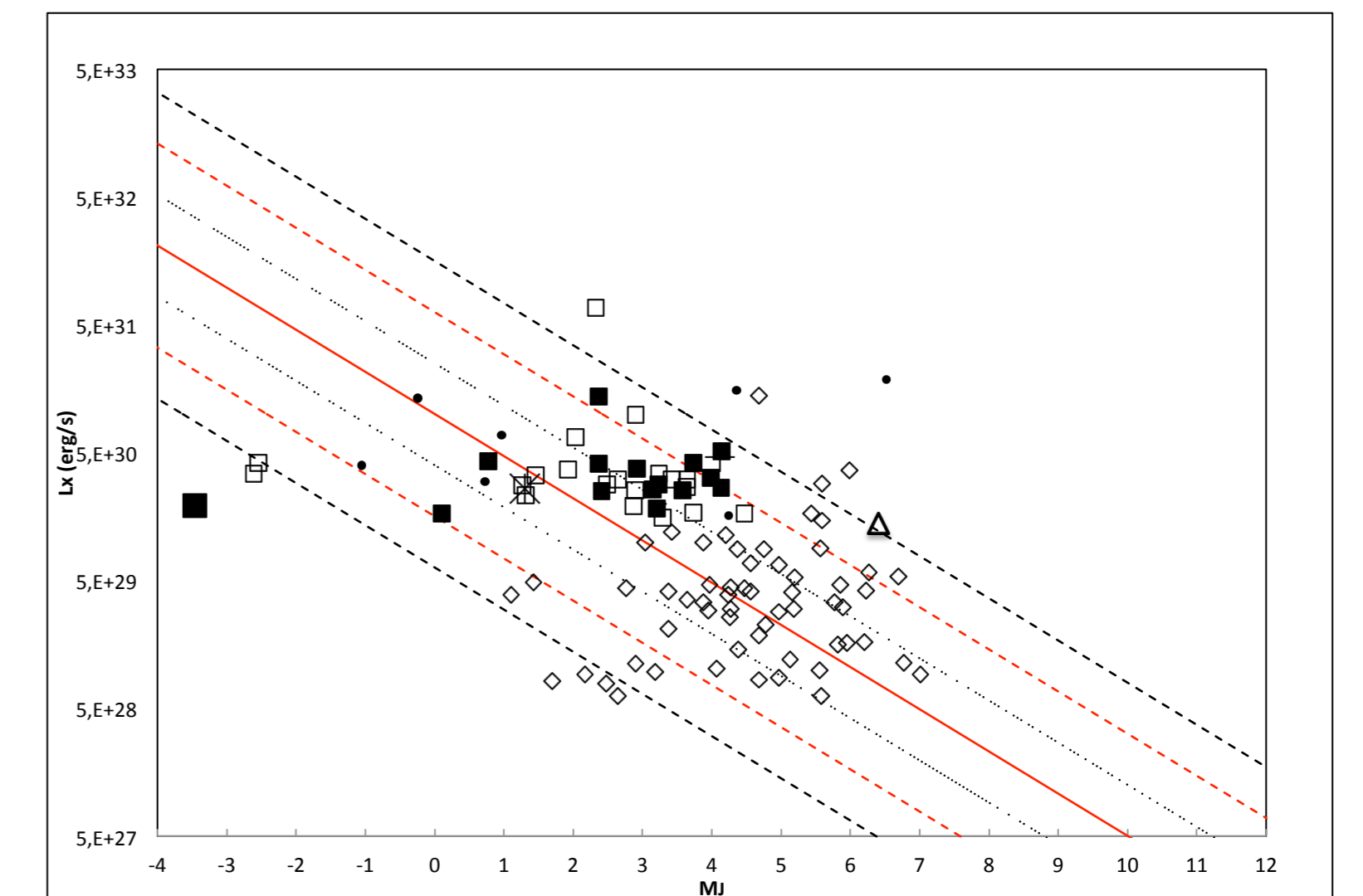


Fig.6.: X-ray luminosity (L_x) v.s. absolute magnitude in 2MASS J band (M_J): the red line represents the relation $\log(L_x) = 31 - 0,33M_J$ found by Gregorio-Hetem et al. (2009) through ROSAT data. Dotted and dashed black lines represent the uncertainties in 1σ and the dashed red line is 2σ ($\alpha = 0,4$ ergs/s). The full and open squares represent the YSO and YSO candidate, crosses and dots are field candidate and field objects respectively, and the galaxy and Herbig Ae/Be identified in our sample are represented by open triangle and star. The open diamonds represent the Chameleon sample (GH2009).

Summary

- ✦ We detected 327 sources in three different energy set ranges. Most of these sources have hardness ratio compatible with young objects, mainly in the east field;
- ✦ The CMD reveals an age of about 5Myrs;
- ✦ 45 spectra of X-ray sources could be evaluated, and for most of the field or field candidates a thermal plasma models could not be fitted.
- ✦ The YSO and YSO candidates of this sample follow the same relation between X-ray and NIR luminosities found by GH2009.
- ✦ 48 sources could be classified: 16 YSOs, 21 YSO candidates, 3 field candidates and 8 field objects.
- ✦ The next step is to apply the same procedure of analysis to the 327 sources in order to completely characterize our whole sample.

References

Barrado, D., Stelzer, B., Morales-Calderón, M., et al. 2011, A&A, 536, 63
 Della Ceca, R., Maccacaro, T., Caccianiga, A., et al. 2004, A&A, 428, 383
 Feigelson, E. D., Montmerle, T. 1999, ARA&A, 37, 363
 Hasinger, G. et al. 2001, A&A, 365, 45
 Gregorio-Hetem, J., Montmerle, T., Rodrigues, C. V., et al. 2009, A&A, 506, 711
 López-Santiago, J., & Caballero, J. A. 2008 A&A, 491, 961
 Montmerle, T.; Grosso, N.; Feigelson, E. D.; Townsley, L., 2002, astro.ph, 6033
 Rieke, G. H., & Lebofsky, M. J. 1985, ApJ, 288, 618
 Siess, L., Dufour, E., & Forestini, M. 2000 A&A, 358, 59